Materials and Design 116 (2017) 278–286; http://dx.doi.org/10.1016/j.matdes.2016.12.010

Processing of preceramic polymer to low density silicon carbide foam

Prasanta Jana*, Emanuele Zera and Gian Domenico Sorarù

Department of Industrial Engineering, University of Trento, Via Sommarive 9, 38123 Trento, Italy

Abstract

A method is described here for preparing lightweight and low cost polymer-derived silicon carbide foam by impregnation of preceramic polymer in polyurethane foam. A series of silicon carbide foams with various density (0.035–0.35 g/cc), porosity (87–98%) and thermal conductivity (0.05–0.12 W/m. K) were prepared using allylhydropolycarbosilane as a base materials. Surface analysis shows that the resultant foams have an open and interconnected porous structure. Phase analysis shows that it is beta silicon carbide with a cubic crystal structure. There was no evidence of cracks or damage even after treating the silicon carbide foam with concentrated hydrofluoric acid for 12 days. From the oxidation resistance experiment, it can be concluded that the silicon carbide foam is stable up to 1500°C in air and 2000°C in argon.

Keywords: Replica method, Polyurethane foam, Polymer-derived ceramics, Silicon carbide foam

*Corresponding author.

E-mail addresses: prasanta.jana@unitn.it

1. Introduction

Open cell reticulated silicon carbide (SiC) foam holds the unique combination of microstructure (porosity from 60% up to 98%, cell size in the microns/millimeters size range) and material properties (high temperature stability, low density and low creep at high temperature, high thermal shock resistance and exceptional chemical inertness). For this reasons, it is suitable for various engineering applications such as the filtration of molten metals or particulates from exhaust gases, radiant burners, catalyst supports, kiln furniture, reinforcement for metals, lightweight sandwich structures, heat sinks etc. [1]. There are many approaches to produce SiC foams: i. replication of sacrificial foam [2, 3], ii. direct foaming [4], iii. burn out of fugitive pore formers [5] and iv. the gelation-freezing method [6]. A comprehensive review on the processing and properties of macroporous SiC has been recently published [7].

It has been proposed that polymer derived ceramics (PDCs) route using preceramic polymers is a promising route for the fabrication of various porous structures (foams, membranes and monolithic components with hierarchical porosity). The polymer-to-ceramic transformation process enabled significant technological breakthroughs in ceramic science and technology. It leads to develop Si-C, Si-O-C and Si-C-N ceramics, which are stable at ultrahigh temperatures with respect to decomposition, crystallization and creep [8–12]. Moreover, several important optical [13, 14], electrical [15–17] and electrochemical [18] properties associated with PDCs have also been reported and exploited for the development of LEDs [19, 20], micro glow plugs [21], pressure sensors [22], pacemaker [23], gas sensors [24] or anodes for Li-ion batteries [25, 26].

For preparing SiC foam through the replica method, most of the studies have been focused on the use of a SiC powder slurry, which is impregnated into the sacrificial template [2–3, 27]. The main limitation of this approach is the very high sintering temperatures needed to consolidate the SiC powders. On the other hand, impregnation of the polyurethane (PU) foam with a preceramic polymer solution does not require very high temperatures for the pyrolysis step and, in principle, could provide an easier, faster and cost effective processing route. However, in spite of these promising features, this method has only been briefly touched by the scientific community [28, 29] and the available papers only seldom report some physical properties of the studied SiC foams [30].

The present work aims to study in details the processing of SiC foam by replication of PU foam by impregnation with a polycarbosilane (PCS) solution and to characterize their

physical and mechanical properties. It is noteworthy to mention that PCS has been extensively utilized as a base material to obtain SiC aerogel or fibres [31, 32]. However, there are few studies concerning the use of PCS to fabricate SiC foam [4, 5] and none of them via replica method from PU foams. Since SiC foams have been proposed for applications in harsh environment (ultra-high temperature and/or aggressive chemical environments), the present work reports also: (i) the oxidation behavior of SiC foam in air up to 1500°C, (ii) the thermal stability in argon up to 2000°C and (iii) the chemical stability in concentrated hydrofluoric acid.

2. Materials and methods

PU foam used in this study was collected from a University waste basket and is referred to as PU foam waste (PUFW). PU foam is widely used in everyday life, however, an efficient means of disposing has not been established yet. There are mainly three means of disposing of PU foam waste: landfill, incineration and recycling. Recycling is obviously the most desirable way. Accordingly, the process of making SiC foam using PUFW may provide an added benefit of recycling. Converting PUFW to carbon foam is one example of recycling [33, 34]. The present work also deals with similar approach to produce SiC foam using PUFW as a replica.

Allylhydropolycarbosilane, SMP-10 (Starfire Systems, Schenectady, USA) was used as received. Platinum–divinyltetramethyldisiloxane complex in xylene, with Pt content of ~2% (Sigma–Aldrich, Saint Louis, MO, USA) was further diluted in xylene to obtain a practical solution containing 0.1 % of catalyst. According to the manufacturer, SMP-10 has an average molecular weight of 5000–25000 and an approximate composition of $–[SiH_2–CH_2]_x–[SiH(allyl)–CH_2]_y–$ in a x:y=9:1 ratio. Cross–linking of polycarbosilane was performed via hydrosilylation reaction of the Si-H bonds of SMP-10 with the SMP-10's allyl groups in presence of the Pt catalyst. In a typical synthesis, SMP-10 was mixed with the solvent (cyclohexane) in the presence of Pt catalyst. The ratio of the volume of the solvent with the volume of the PUFW was kept constant to $\frac{1}{5}$ for all the studied materials. For example, for 10 cc PUFW sample, 2 cc of solvent was used. The impregnation process has been carried out by manually squeezing the flexible PUFW into the solution and releasing it, so that all the solution was sucked into the foam pores. This process has been repeated several times to ensure that the foam was homogeneously wet and no solution was left in the container. Several samples have been prepared with different SMP-10/PUFW mass ratios

ranging from 0.5 up to 8. The impregnated PUFW was then left to dry at room temperature for one day and then pyrolyzed in a tubular furnace (Lindbergh Blue) at 2°C/min up to 1200°C and 1500°C with 2 h dwell time at the maximum temperature under nitrogen flow (100 cc/min). The furnace tube was purged for 5 h with nitrogen before pyrolysis to remove traces of oxygen and moisture. The SiC foam prepared at 1200 °C was also further heated to 2000°C in flowing argon (100 cc/min) in an Astro graphite furnace (Thermal Technology). Flowchart for preparing SiC foam is shown in **Figure 1**.

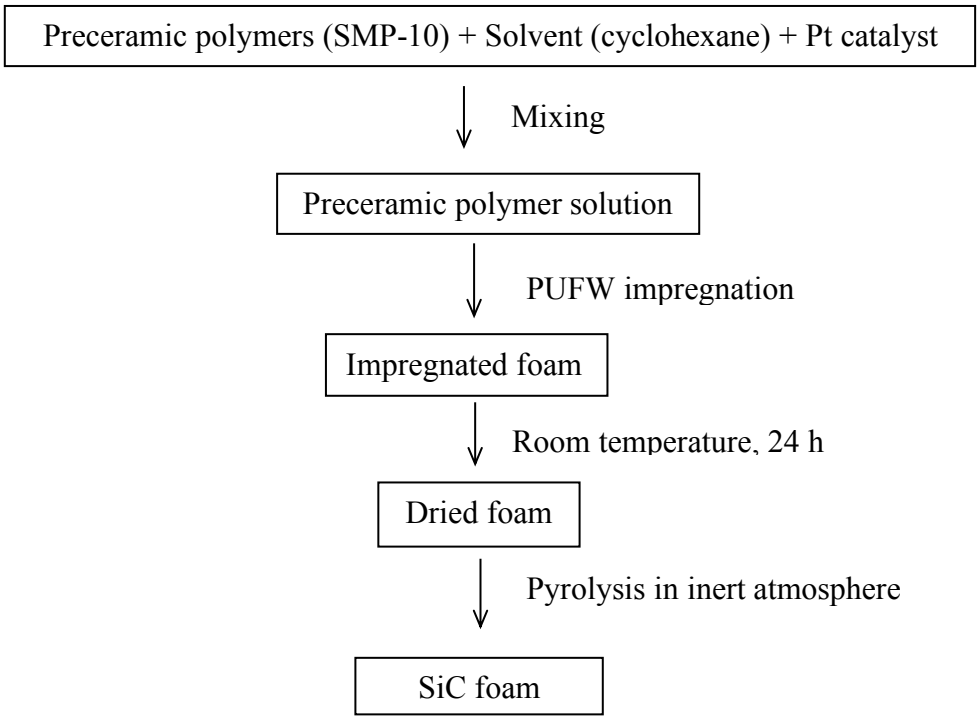

Figure 1. Flowchart for the preparation of SiC foam.

The shrinkage of foam samples during pyrolysis was calculated by measuring the dimensions of foams with a digital caliper. The mass loss associated with the polymer-to-ceramic transformation was measured with the help of microbalance. These measurements allow to calculate the bulk density (ρ_b) before and after pyrolysis. The skeletal density (ρ_s) was measured using a Micromeritics 1305 helium pycnometer (Micromeritics, Norcross, GA, USA). From the bulk and skeletal densities, the percentage of porosity, P (dimensionless) of the materials was also calculated.

Surface morphology of the foams was examined using a scanning electron microscope (SEM, Jeol-JSM-5500) after Au film deposition by sputtering. Individual cell and

window sizes were measured by using Image-Pro Plus software, based on several images per sample, from which average cell, window and strut sizes were calculated.

The crystallinity of the SiC foams (pyrolysised at 1200–2000°C in inert atmosphere) was analyzed by X-ray diffraction (XRD) pattern with a Rigaku D/Max diffractometer (Rigaku, Tokyo, Japan) in the Bragg–Brentano configuration. The XRD patterns were recorded in the angular range 10–80° with a step size 0.05° and 5s acquisition time using monochromatic X-rays. For the phase analysis after air oxidation of the SiC foams, XRD data was acquired on an Italstructures IPD3000 instrument equipped with a Cu anode source (line focus), a multilayer monochromator to suppress k-beta radiation and fixed 100 μm slits. The sample was positioned in reflection geometry with a fixed angle with respect to the incident beam, and spectra were collected by means of an Inel CPS120 detector over + 120° two-theta range.

Thermal conductivity measurements were carried out at room temperature by the transient plane source method (Hot Disk TPS 2500 S, city= do we need to put it?). The method is based on a transiently heated plane sensor, used both as a heat source and as a dynamic temperature sensor. It consists of an electrically conducting pattern in the shape of a double spiral, which has been etched out of a thin nickel foil and sandwiched between two thin sheets of Kapton®. The plane sensor was inserted between two well-fitted parallelepiped pieces of sample, each one with a plane surface facing the sensor. The thermal conductivity was then calculated with the Hot Disk 6.1 software.

Mechanical properties (elastic modulus and compressive strength) were tested on cubic samples (3 × 3 × 3 cm) with a MTS 810, MTS systems corp, ~~14000 Technology Drive~~, Eden Prairie MN, USA, 55344?? with a force transducer of 1 kN (precision of 0.1 % over full scale) using a deformation rate of 1 mm/min.

To test the high temperature stability in oxidative environment, cubic samples (15 x 15 x 15 mm) of SiC foam obtained at 1200°C were also heated at 10°C/min in air up to 1200, 1300 and 1500°C with 10 h dwell time at the maximum temperature and free cooling in the furnace to room temperature. After the oxidation treatment, the foams have been characterized by measuring the mass gain/loss and the compressive strength. The crystallinity of the oxidized foams has been checked by XRD.

The chemical durability experiments were conducted by soaking SiC foam in 48% concentrated HF solution for 12 days at room temperature and measuring the mass loss of the samples.

3. Results and discussion

Foam samples have been prepared using different SMP-10/PUFW mass ratios in the range 0.5–8. The structural and microstructural characterization has been, in general, performed on samples prepared using a ratio SMP-10/PUFW= 1 while the physical properties (density, porosity, thermal conductivity and compressive strength) have been measured on the whole set of samples.

As mentioned earlier, main idea to use PU foam waste is to reuse the waste to prepare SiC foam. PU foams are produced in large amounts and there is a growing interest in finding suitable recycle processes [33, 34]. Details of the characterization of the PUFW was reported elsewhere [35, 36]. For example, in order to select the proper heating schedule for the processing of the ceramic foams, the behavior during pyrolysis of a sample of PUFW was previously studied. The PUFW heated in N_2 flow showed a maximum decomposition at 490°C and at 1100°C, a total weight loss of ~97% with a ~3% carbon residue [36]. PUFW shows a glass transition temperature determined by the DSC at –61°C [35]. Commercial polyurethane foam belongs to two main types: ester– and ether–based. From the FT-IR studies, it was concluded that the used PUFW was an ether–based type [36].

3.1 Characterization of the impregnated PUFW samples

Figure 2 shows the SEM images of PUFW before and after SMP-10 impregnation. PUFW (as shown in **Figure 2a** and **2b**) shows nearly hexagonal cells with oval windows and smooth struts. The average cell, window and strut sizes were found to be 724, 266 and 77 μm, respectively. After SMP-10 impregnation (as shown in **Figure 2c** and **2d**), PUFW exhibits similar microstructure with no appreciable change in cell and window size and shape. However, the surface of the strut became corrugated.

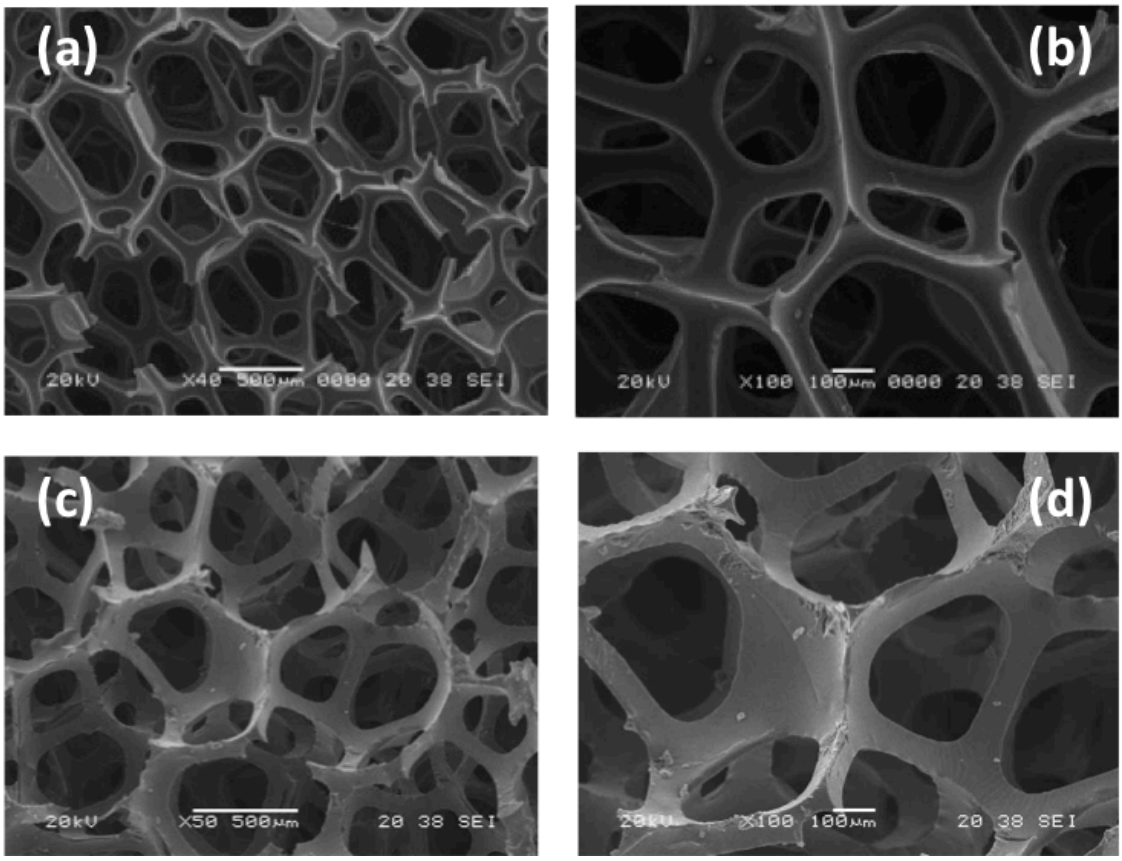

Figure 2. SEM images of (a) and (b) starting PUFW, (c) and (d) PUFW after SMP-10 impregnation (SMP-10/PUFW = 1).

The impregnation process consisted of wringing the PUFW several times (by hand) in the solution of preceramic polymer and then releasing the foam in such a way that it could absorb the solution completely within its open cells. This ensures that the solution of preceramic polymer permeates evenly throughout entire volume of the PU foam network. It is plausible that the preceramic polymer solution can swell the PUFW structure and when the solvent evaporates, the crosslinked preceramic polymer is retained in between the PUFW molecular structure for the subsequent pyrolysis step. The presence of the crosslinked Si-containing polymer in the impregnated PUFW was already proven by FT-IR in a previous work [35]. However, FT-IR analysis is not able to ascertain if the polycarbosilane is present as a coating on the surface of the struts or if SMP-10 is also present in the bulk of the struts, between the PUFW molecular chains. The answer of this question can be found by studying, with SEM, the fracture surface of the impregnated foam. Typical fracture surfaces obtained after soaking the PUFW in liquid nitrogen are reported in **Figure 3**. Before impregnation, the PUFW shows a smooth fracture surface typical of a brittle material, **Figure 3(a)**, while the

PUFW impregnated with the SMP-10, **Figure 3(b)**, shows a corrugated fracture surface suggesting a more ductile behavior. This result can be rationalized thinking that SMP-10 is present between the polyurethane chains and acts as a plasticizer. Another, more direct, evidence of the presence of the Si-polymer in the bulk of the foam struts arises from the results of the EDX line scan of Si shown in the inset of **Fig. 3(b)**. It can be appreciated that Si is present in high concentration at the surface as well as in the bulk of the struts.

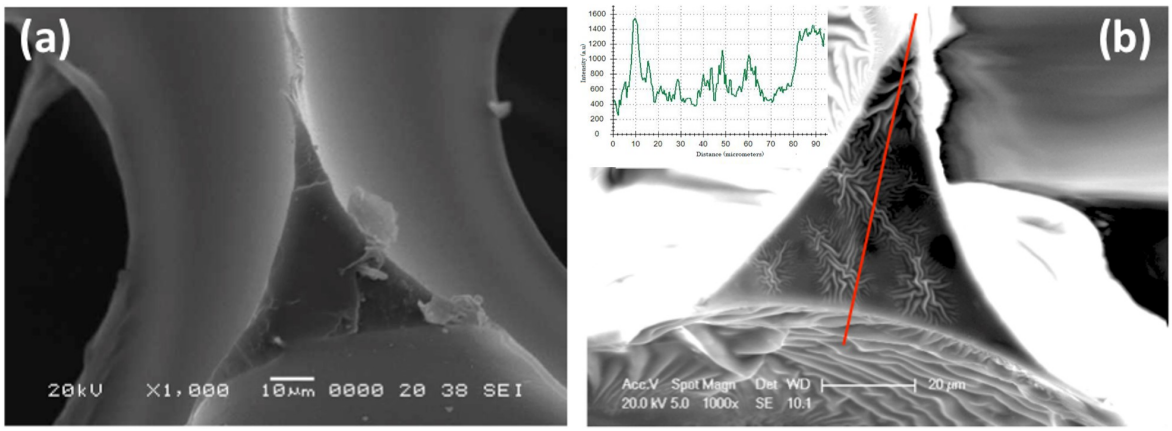

Figure 3. SEM images of (a) PUFW and (b) PUFW impregnated with SMP-10 (SMP-10/PUFW = 1). The inset in Figure 3(b) shows the Si EDX line spectrum.

3.2 Characterization of the foams during pyrolysis

Figure 4 shows the photographs of PUFW transforming into SiC foams at various stages of the pyrolysis process.

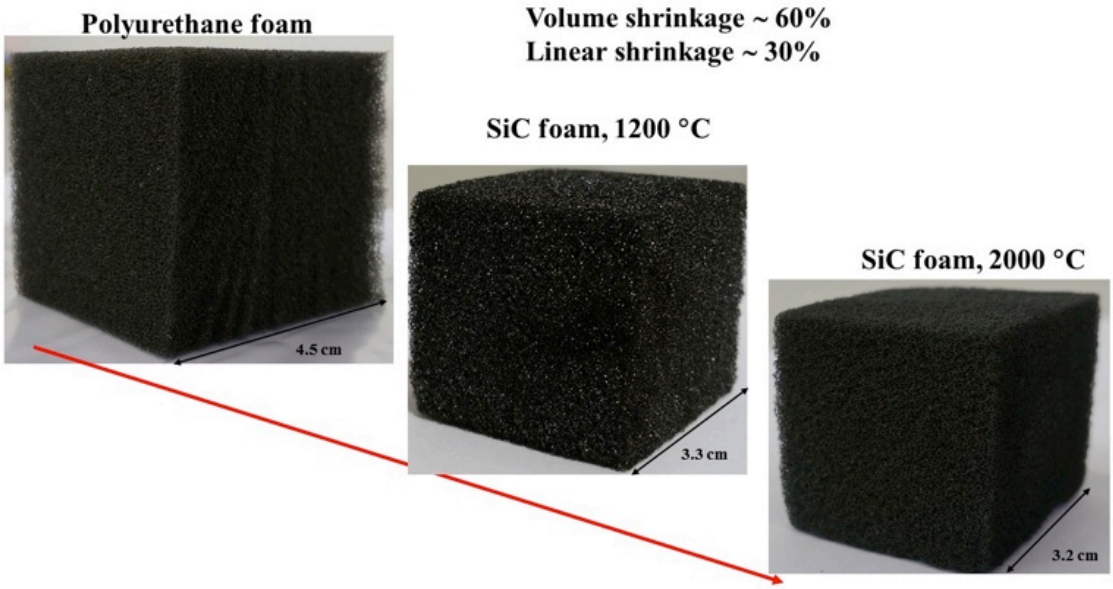

Figure 4. Photographs of PUFW transforming into SiC foam (SMP-10/PUFW = 1).

Figure 5 shows SEM images presenting the microstructure of the resultant SiC foam (pyrolyzed at 1200°C). As previously stated, the average cell, window and strut sizes of the PUFW were found to be 724, 266 and 77 µm, respectively. After converting PUFW to SiC foam, morphology of the SiC foam is a perfect replica of the PUFW, however with a smaller cell (495 µm), window (172 µm) and strut sizes (56 µm). From the SEM analysis, it can be concluded that shrinkage of cell, window and strut sizes are ~32, 35 and 27%, respectively. These values compare very well with the macroscopic shrinkage of the foam (~30%) which was obtained by measuring the dimensions of foams with a digital caliper. One interesting observation is that the linear shrinkage is ~30% for all SiC foams synthesized by various SMP-10/PUFW mass ratios. This result suggests that the shrinkage during pyrolysis is controlled by the shrinkage of the SMP-10, which is, indeed, close to 30% [37]. It is noteworthy to mention that the struts of the SiC foam (shown in SEM image made at higher magnification, **Figure 5**) are dense. As it is mentioned earlier, it is due to the crosslinked SMP-10 retained in between the PUFW molecular structure and during pyrolysis, the PUFW decomposes while the SMP-10 transforms into the SiC leading to the formation of dense struts.

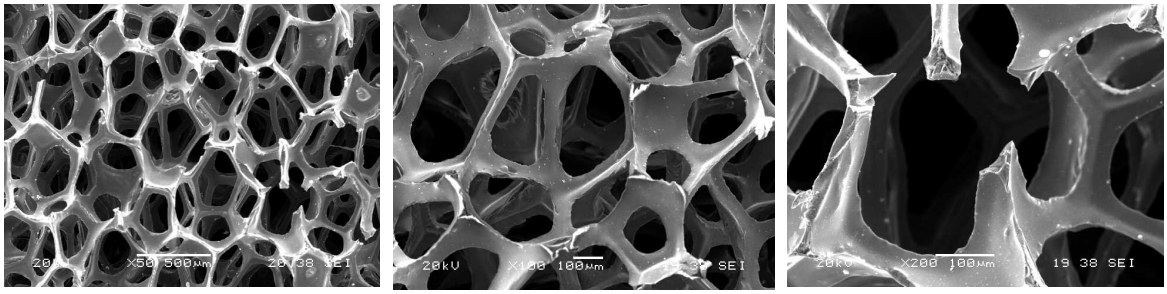

Figure 5. SEM images of the resultant SiC foam (SMP-10/PUFW = 1) pyrolyzed at 1200°C.

Table 1 – Physical properties of the SiC foam (SMP-10/PUFW = 1) pyrolyzed at 1200°C.

Density (g/cc)	Mass loss (%)	Linear shrinkage (%)	Cell size (µm)	Window size (µm)	Strut size (µm)
0.07	54	30	495	172	56

Figure 6 shows XRD patterns of SiC foam pyrolysed at 1200, 1500 and 2000°C. At 1200°C, the XRD spectrum shows broad diffraction peaks at 35°, 60° and 72° corresponding to nanocrystalline cubic silicon carbide (β–SiC). Increasing the temperature to 1500°C and then up to 2000°C leads to a sharpening of the diffraction peaks and at 2000°C, a well crystallized β–SiC foam is formed. This indicates the phase stability of the SiC foam even at very high temperature.

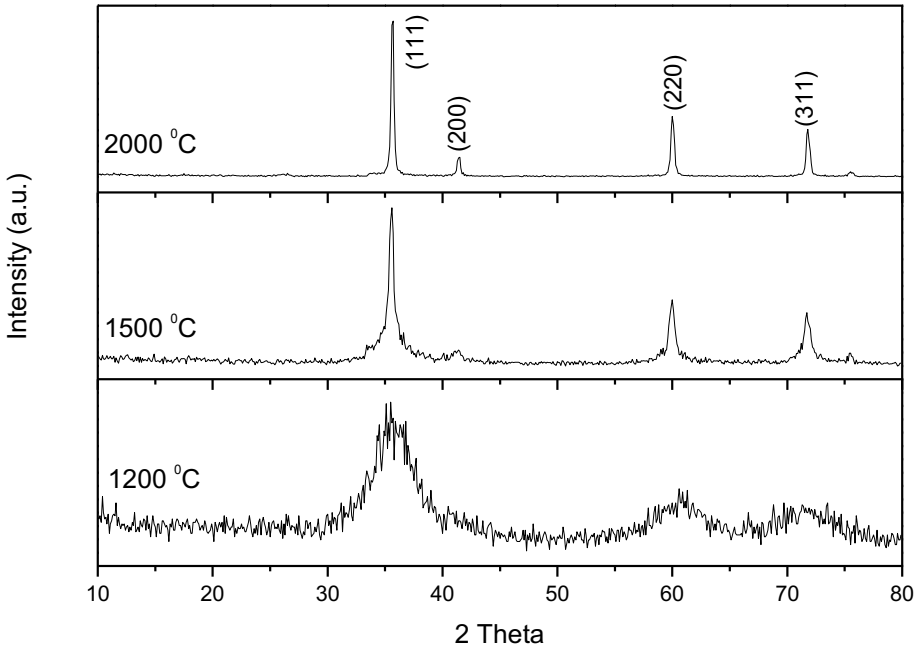

Figure 6. XRD pattern of SiC foams (SMP-10/PUFW= 1) pyrolyzed in N_2 flow at 1200°C, 1500°C and 2000°C (in argon flow).

3.3 Characterization of the physical properties of the SiC foams

3.3.1 Density, porosity and thermal conductivity

The bulk density, skeletal density, porosity and thermal conductivity values of SiC foams processed with different SMP-10/PUFW mass ratios and pyrolyzed at 1200°C are reported in **Table 2**. Data shown in **Table 2** reveals that the density and thermal conductivity of the SiC foams can be easily changed by varying the mass ratio between the preceramic polymer SMP-10 and PUFW. For example, the density can be increased by 10 times (0.035 g/cc to 0.35 g/cc) and the thermal conductivity from 0.05 W/m. K to 1.2 W/m. K (2.4 times) when the mass ratio between SMP-10 and PUFW is increased from 0.5 to 8. The thermal conductivities of the SiC foams are in the range 0.05–0.12 W/m. K i.e. much lower than

similar SiC foams present in the market [38], which are known to be highly insulating materials for the application at ultra-high temperatures. This difference most probably is related to the difference in processing method, which results into a material with a different microstructure. The SiC foam reported in the reference [38] is probably obtained by CVD method (depositing SiC on a carbon foam). Accordingly, the carbon core present in the struts could be responsible for the higher thermal conductivity compared to the present SiC foam.

Table 2 – Density, porosity and thermal conductivity of SiC foams pyrolyzed at 1200°C.

SMP-10 : PUFW	Bulk Density (g/cc)	Skeletal density (g/cc)	Porosity (%)	Thermal conductivity (W/m. K)
0.5:1	0.035	2.03	98	0.05
1:1	0.07	2.24	97	0.06
2:1	0.11	2.31	95	0.07
3:1	0.16	2.41	93	0.08
4:1	0.21	2.54	92	0.10
6:1	0.28	2.63	89	0.10
8:1	0.35	2.72	87	0.12

To fit thermal conductivity with density ratios of the SiC foam, Gibson–Ashby model [39] was also applied. It anticipates a linear dependence of the thermal conductivity of the SiC foam with the density ratios as shown in the following equation,

$$k_{SiC\ foam} = \frac{1}{3}\left(\frac{\rho_b}{\rho_s}\right)k_{SiC} + \left(1 - \frac{\rho_b}{\rho_s}\right)k_{air}$$

that can be re-written as,

$$k_{SiC\ foam} = \left(\frac{1}{3}k_{SiC} - k_{air}\right)\frac{\rho_b}{\rho_s} + k_{air}$$

Where $k_{SiC\ foam}$ is the thermal conductivity of the SiC foam, k_{SiC} is the thermal conductivity of the SiC struts, k_{air} is the thermal conductivity of the air (0.025 W/m. K), ρ_b is bulk density of SiC foam and ρ_s is skeletal density of SiC. The variation of thermal conductivity with respect to density ratios of the SiC foams is shown in **Figure 7**. The experimental results show a good linear dependence of the thermal conductivity from the density ratio, as predicted by the Gibson–Ashby model. The intercept of the fit with the Y-axis determines the thermal conductivity value for the air, which is slightly higher than the usual reported value

(0.04 vs 0.025 W/m. K). From the slope of the linear fit, the thermal conductivity of the PDC SiC can be evaluated as ~1.7 W/m. K. The thermal conductivity of PDC SiC was only recently reported in the literature for a dense sample pyrolyzed at 1800°C (8.4 W/m. K) [40] and for porous bodies pyrolyzed at temperatures in the range 1200 up to 1800°C [41]. In the inset of **Figure 7**, the thermal conductivity values of the SiC foams have been plotted together with the thermal conductivity reported in the literature for a porous PDC SiC pyrolyzed at the same temperature (1200°C) as in the present work. The porous PDC SiC from the literature [41], showed a relative density of 0.53 and a thermal conductivity of 0.5 W/m. K. The linear fit is still proving that the Gibson–Ashby model is valid over a large range of density ratios. From this fit, the estimated value of thermal conductivity of air is ~0.02 W/m. K (closer to the usual value reported in the literature) and k_{SiC} is ~2.7 W/m. K. Considering these results all together, it can be concluded that the thermal conductivity of PDC SiC pyrolyzed at 1200°C is in the range 1.7–2.7 W/m. K. The lower values estimated in the present work compared with the thermal conductivity reported in the literature for dense PDC SiC (1.7–2.7 vs 8.5 W/m. K) can be rationalized as follows. In the present study, the PDC SiC samples were pyrolyzed at a lower temperature leading to a polycrystalline SiC with smaller grain size and presumably higher defect concentration resulting in higher phonon scattering and hence it leads to lower thermal conductivity. Moreover, the strong dependence of thermal conductivity with respect to maximum pyrolysis temperature for a PDC SiC was observed. It is shown that increasing the pyrolysis temperature of a porous PDC SiC from 1200 up to 1800°C increases the thermal conductivity of almost 6 times from 0.5 to 2.8 W/m. K [41].

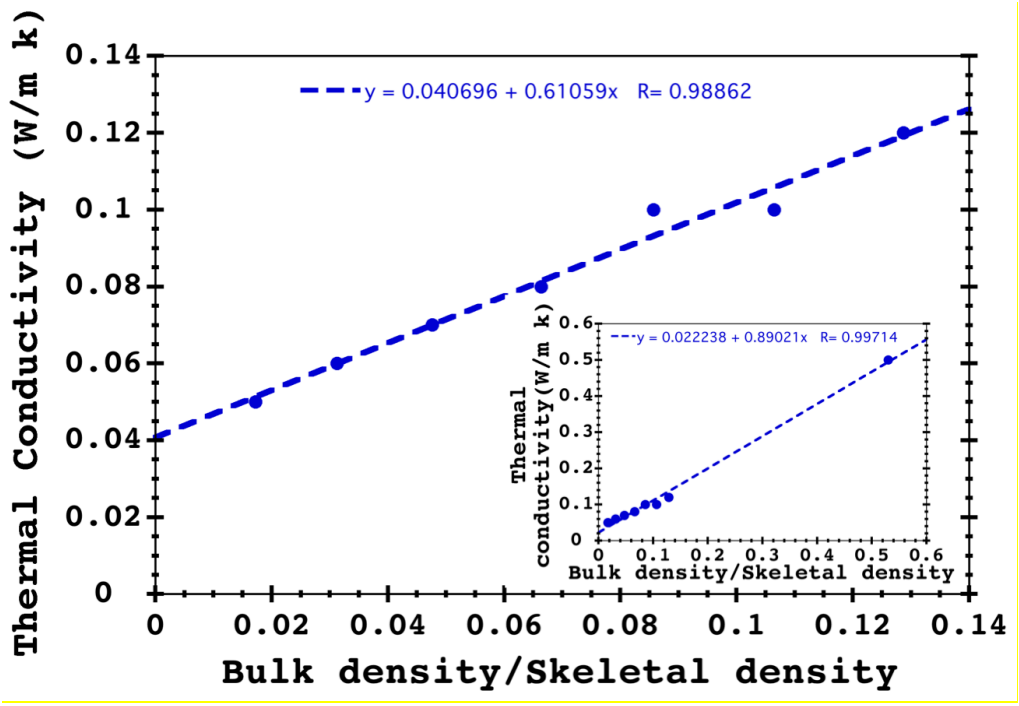

Figure 7 Variation of thermal conductivity of the SiC foams as a function of density ratio. In the inset, the plot has been redrawn including the result of the thermal conductivity of a porous PDC SiC with a density ratio of 0.53 [40].

3.3.2 Mechanical properties

Mechanical properties (compressive strength and elastic modulus) were measured on SiC foams pyrolyzed at 1200°C (prepared with different SMP-10/PUFW mass ratios). Typical stress–strain curve is shown in **Figure 8**. The stress–strain diagram of the SiC foam samples are highly serrated, due to the successive ruptures of the struts undergoing compression, but still exhibit two distinct regions: one linear up to ~10% strain and a plateau up to ~70% strain. From these curves, the corresponding compressive strengths and elastic moduli have been determined and reported in **Table 3**. The elastic modulus has been evaluated from the slope of the linear region while the compressive strength has been determined as the central value of the plateau region as shown in **Figure 8**. Compressive strength and elastic modulus values are within the range 0.17–0.75 MPa and 2.7–11.7 MPa, respectively.

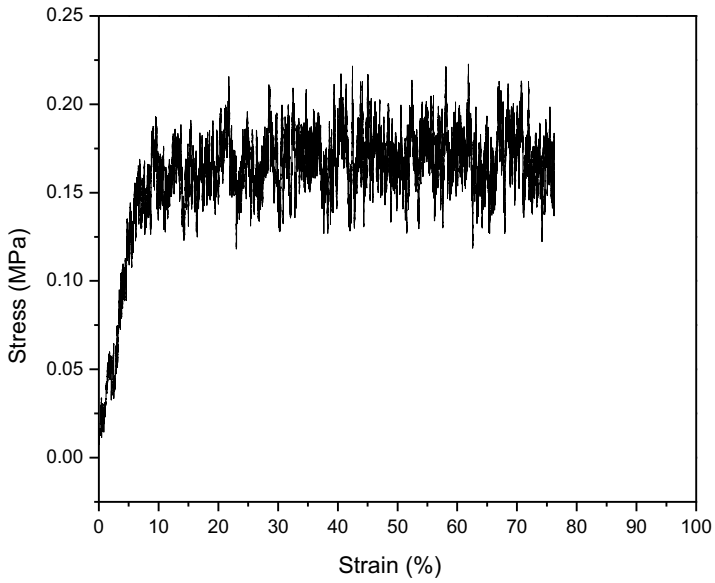

Figure 8. Stress-strain characteristics of SiC foam with 97% porosity.

Table 3 – Mechanical property of SiC foams pyrolyzed at 1200°C.

SMP-10:PUFW	Porosity (%)	Compressive strength (MPa)	Elastic modulus (MPa)
1:1	97	0.17	2.7
2:1	95	0.26	6.2
3:1	93	0.30	7.2
4:1	92	0.46	9.3
8:1	87	0.75	11.7

Compressive strength of the SiC foam as a function of the (density ratio)$^{2/3}$ as proposed by the Gibson-Ashby model [39] for fracture dominated behavior of brittle foam was also analyzed by using following equation.

$$\sigma_{SiC\ foam} = C\ \sigma_{SiC}\ (\frac{\rho_b}{\rho_s})^{3/2}$$

In this formula, $\sigma_{SiC\ foam}$ is compressive strength of the SiC foam, σ_{SiC} is bending strength of the SiC ligaments and C is 0.2 given by Gibson-Ashby model. **Figure 9** shows the variation of compressive strength with (density ratio)$^{2/3}$ and it suggests that indeed compressive strength of the SiC foam follow the Gibson–Ashby model pretty well.

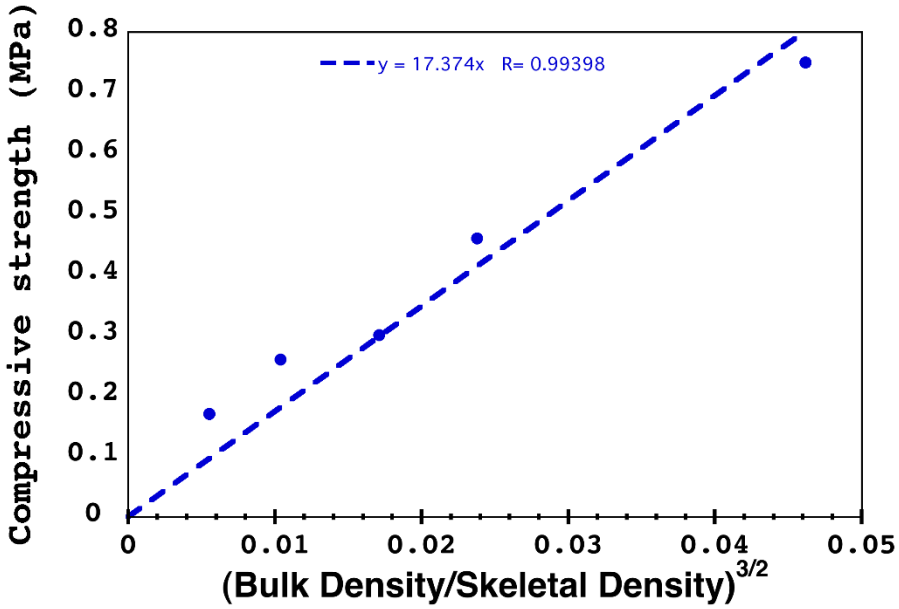

Figure 9 Variation of $\sigma_{SiC\ foam}$ with respect to $(\frac{\rho_b}{\rho_s})^{3/2}$.

From the linear fit, the bending strength of the SiC struts is estimated as: σ_{SiC} = 87 MPa. In the literature, the bending strength of dense, PDC ceramics is rarely reported due to the well-known difficulty in processing of dense, crack-free samples suitable for this type of measurement. Actually no values can be found for PDC SiC and only few papers report the bending strength of similar dense, crack-free PDC samples belonging to the SiOC and SiCN systems. For the SiOC system, values in the range 80–500 MPa, depending from the composition and the maximum pyrolysis temperature, have been reported by different authors [42–44] while only one paper reports the bending strength of SiCN which is found in the range 400–500 MPa [45]. Therefore, even if the bending strength value found in this study seems to fall in the lower side of the bending strength range of PDCs, the obtained bending strength value is still consistent with the available literature.

The SiC foams reported in this study encompasses a porosity range (from 87 up to 98 vol%) which is rarely reported in the literature for SiC as well as other porous ceramic materials. As mentioned in the introduction, a comprehensive review on the processing and properties of macroporous SiC has been recently published [7]. In this review many properties like thermal conductivity, compressive strength, etc., are compared with the porosity of the samples in the range 30–90%. It can be easily appreciated that the range of porosity investigated in present study is far beyond the most studied ones.

Very few papers dealing with high porosity SiC [3, 27] was reported. Yao et al. [27] synthesized SiC foam by the replica method using PU foams and ceramic slurries containing SiC and Al_2O_3 powder, sintered at 1300°C. The reported compressive strength of the resulting SiC foam having 89% porosity was 0.32 MPa. Mouazar et al. [3] reported compressive strength (0.07 MPa) of a SiC foam (porosity 88%) prepared by replica method using SiC powder slurry. In the present work, SiC foam with similar porosity (88%) displayed higher compressive strength (0.75 MPa). This can be rationalized knowing that the processing procedure used in this study leads to the formation of dense struts which are stronger then the hollow struts obtained from the conventional replica technique using ceramic slurries.

Finally, it was observed that, after the compressive test with a total strain of ~70%, the SiC foam did not fully collapse and a small piece of SiC foam remained barely undamaged. This observation suggests that synthesized SiC foam should have a very good machinability and, indeed, SiC foam can be easily machined into different shapes as shown in **Figure 10**.

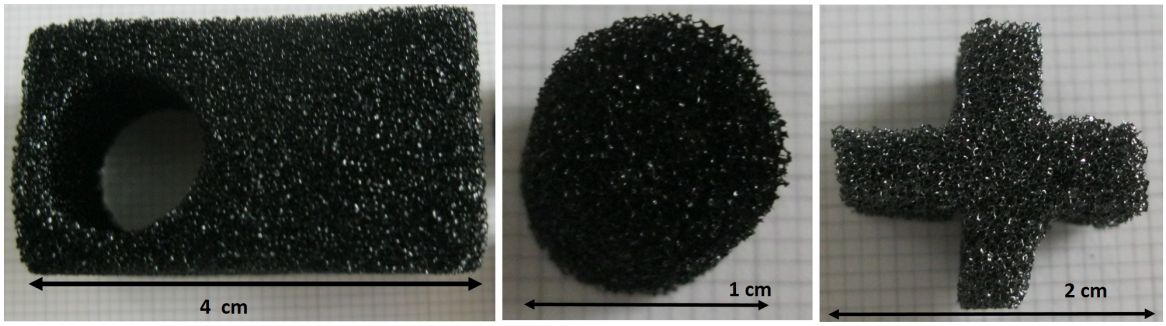

Figure 10. Photographs of SiC foam machined into various shapes.

3.4 Evaluation of the stability of SiC foams in harsh environments: (1) high temperature oxidation and (2) concentrated hydrofluoric acid treatment

Since SiC foams are usually intended for many applications at ultra-high temperature, including as light-weight structural components [46] or for filtering strong acid/basic water solutions, it was decided to test the behavior of SiC foams in oxidative environment (air) up to 1500°C and in concentrated HF water solution (48%) at room temperature. The oxidation resistance of SiC foam was studied with the help of high temperature furnace in air and by measuring the mass change and the compressive strength after the high temperature treatment. The results of the mass change upon oxidation are shown in **Figure 11**.

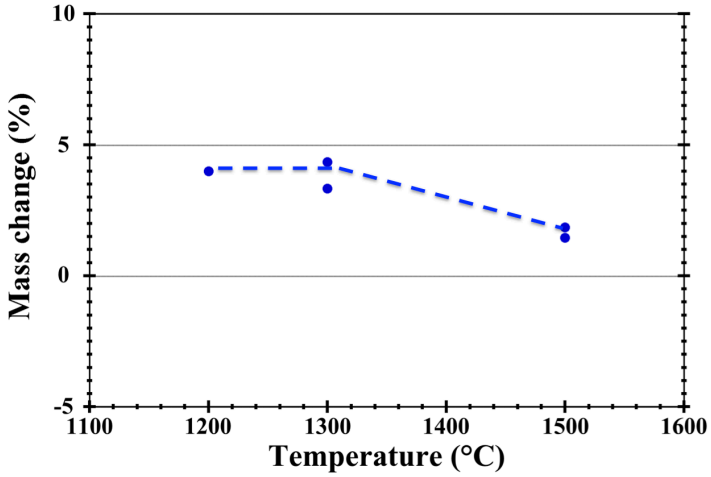

Figure 11. Mass change of SiC foams (porosity 95%) upon 10 h oxidation in air in the temperature range 1200–1500°C.

Up to 1300°C, SiC foam showed around 4% mass increase due to the formation of a SiO_2 passivation layer according to the reaction: $SiC + 2O_2 \rightarrow SiO_2 + 2CO$. Above 1300 °C, the mass increase is lower. This is most probably due to the simultaneous occurrence of the decomposition of a silicon oxycarbide (SiOC) phase which is known to take place in the 1400–1500°C temperature range. The presence of traces of oxygen in the SiC foam, which was previously shown by FT-IR analysis [35], is due either to a reaction during pyrolysis with O_2 impurities in the furnace or with the decomposition products of the PUFW. The formation, upon oxidation, of a thin silica film on the struts of the SiC foam leads to appearance of nice interference colors as shown in **Figure 12**. As a general trend, the color change from bluish to green to reddish by increasing the oxidation temperature/time, in agreement with the expected increase of the silica thickness. No cracks in the SiC foam are visible after the oxidation treatments.

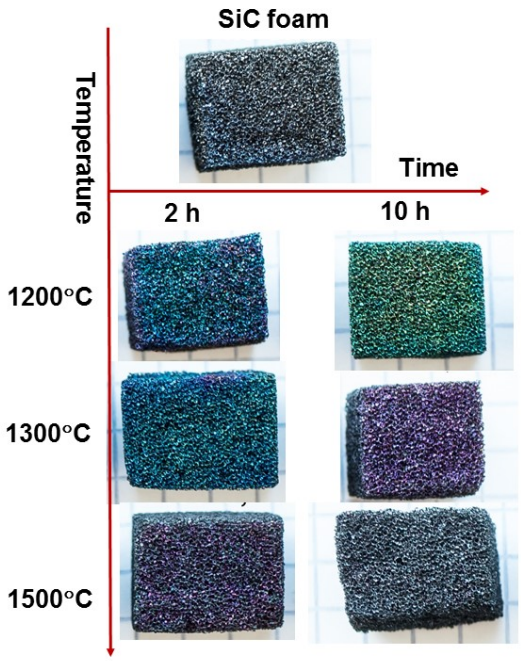

Figure 12. Photographs of SiC foams after air oxidation.

The XRD spectra recorded on the samples oxidized for 10 h at high temperature are reported in **Figure 13**. XRD spectra shows the presence of a sharp peak at ~2θ= 22 ° after the high temperature treatment in air atmosphere, which leads to the formation of SiO_2. The intensity of the SiO_2 peaks increases with the annealing temperature. Shape and size of SiC peaks did not change too much indicating the SiC nanocrystals did not grow significantly.

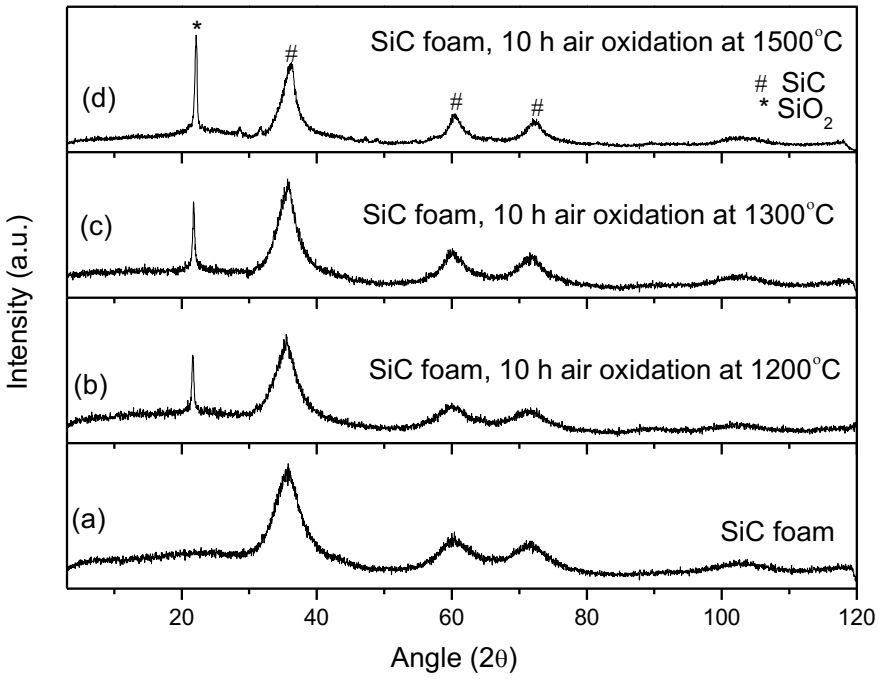

Figure 13. XRD of the starting (a) SiC foam and after oxidation in air for 10 hours at (b) 1200, (c) 1300 and (d) 1500°C.

Compressive strength of the SiC foam (porosity 95%) was also measured after the oxidation treatment in air at high temperature (1200°C–1500°C) as shown in **Figure 14**. Compressive strength of the SiC foam was constant (0.2 MPa) up to 1300°C and thereafter, it slightly reduces, however after 10 hours oxidation at 1500°C, the SiC foam still display a compressive strength of 0.13 MPa which is still higher than pristine SiC foams of comparable (or lower) porosity [3]. The strength decrease observed at 1500°C may be associated with the carbothermal reduction of the SiOC phase which can lead to the development of porosity in the foam struts.

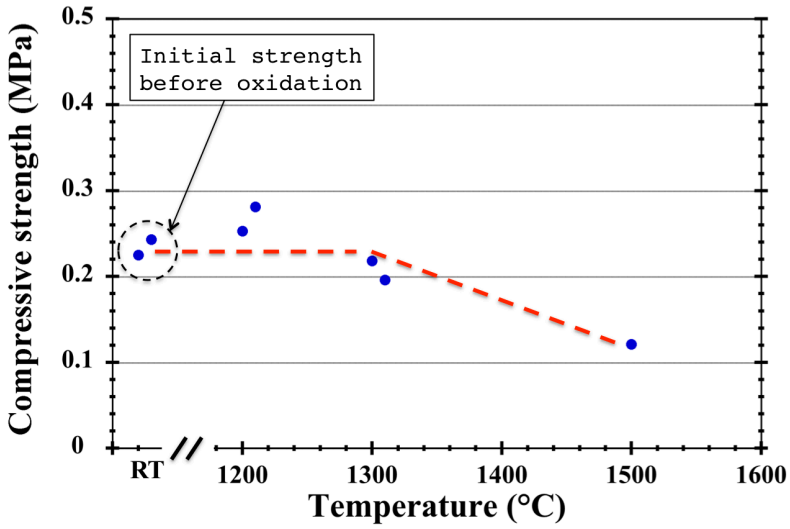

Figure 14. Compressive strength of the SiC foam (porosity 95%) after air oxidation (1200°C–1500°C).

The stability of SiC foams was evaluated by annealing the SiC foam to 2000°C in argon atmosphere. The sample's mass did not change appreciably and the only difference between the two samples was a slight color change: at 2000°C, the SiC foam turned grey as shown in **Figure 4**. These results confirm the structural stability of SiC foam even at very high temperature.

Durability of the SiC foams prepared at 1200°C was evaluated by soaking the foams in concentrated HF (48%) at room temperature for 12 days. There was no visible damage, however, a mass loss of around 5% was observed.

Finally, the synthesis route is also validated by another type of polyurethane template (30 PPI, kindly supplied by ARE S.r.l, Italy) as reported in **Figure 13** which shows similar results.

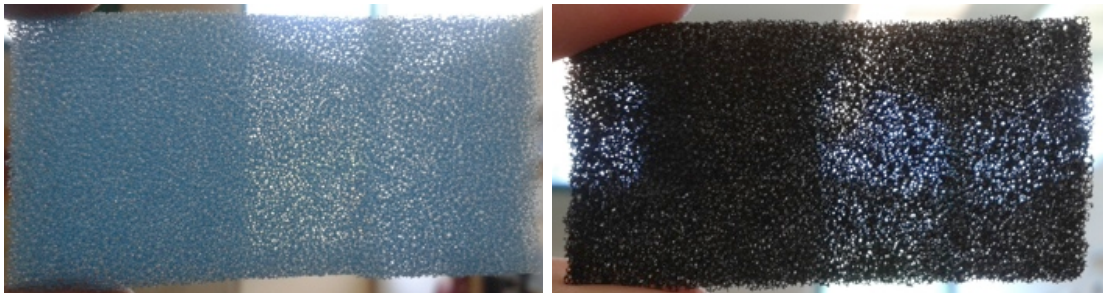

(a) (b)

Figure 13. Photographs of (a) polyurethane foam and (b) resultant SiC foam (1200°C).

The cost of SiC foam is roughly estimated taking consideration the cost of raw materials required for laboratory scale preparation and it should be approximately 10–100 USD per cubic inch, which is much cheaper than market available SiC foam [47].

4. Conclusions

A cost effective and simple process for producing SiC foam was presented. The SiC foams have low density and are highly porous. The resulting SiC foam shows low thermal conductivity which means that it is more thermally insulating than comparable commercially available SiC foams. SEM images of the SiC foam shows an open cells structure made of solid interconnected struts. XRD patterns of SiC foam pyrolyzed at 1200°C, 1500°C and 2000°C showed diffraction patterns corresponding to β–SiC, with a cubic crystal structure. The SiC foam shows very good machinability. It can be concluded that SiC foam (pyrolyzed at 1200°C in N_2) is stable in reactive environment (air oxidation upto 1500°C and in concentrated HF solution).

Acknowledgements

The authors gratefully acknowledge the financial support of European Community FP7 through MC-ITN FUNEA–Project 264873 and Fondazione Cassa di Risparmio di Trento e Rovereto under the contract: Polymer-derived ceramics with hierarchical porosity for water

filtration/purification (project number 2015.0174). The authors also thank Mr. Marco Busato for air oxidation study of the SiC foams and Dr. Mauro Bortolotti for XRD measurements.

References

1. P. Colombo, Conventional and novel processing methods for cellular ceramics, Phil. Trans. R. Soc. A 364 (2006) 109–124.
2. X. Zhu, D. Jiang, S. Tan, Preparation of silicon carbide reticulated porous ceramics, Mater. Sci. Eng. A 323 (2002) 232–238.
3. R. Mouazer, S. Mullens, I. Thijs, J. Luyten, A. Bueckenhoudt, Silicon Carbide Foam by the Polyurethane Replica Technique, Adv. Eng. Mater. 7 (2005) 1124–1128.
4. M. Fukushima, P. Colombo, Silicon carbide-based foams from direct blowing of polycarbosilane, J. Europ. Ceram. Soc. 32 (2012) 503–510.
5. M. Kotani, K. Nishiyabu, S. Matsuzaki, S. Tanaka, Processing of polymer-derived porous SiC body using allylhydridopolycarbosilane (AHPCS) and PMMA microbeads, J. Ceram. Soc. Jap. 119 (2011) 563–569.
6. M. Fukushima, M. Nakata, Y. Zhou, T. Ohji, Y. Yoshizawa, Fabrication and properties of ultra highly porous silicon carbide by the gelation–freezing method, J. Europ. Ceram. Soc. 30 (2010) 2889–2896.
7. J.-H Eom, Y.-W. Kim, S. Raju, Processing and properties of macroporous silicon carbide ceramics: A review, J. Asain Ceram. Soc. 1 (2013) 220–242.
8. S. Yajima, Y. Hasegawa, K. Okamura, T. Matsuzawa, Development of high tensile strength silicon carbide fibre using an organosilicon polymer precursor, Nature 273 (1978) 525–527.
9. R. Riedel, G. Passing, H. Schönfelder, R.J. Brook, Synthesis of dense silicon–based ceramics at low temperatures, Nature 355 (1992) 714–717.
10. T. Ishikawa, Y. Kohtoku, K. Kumagawa, T. Yamamura, T. Nagasawa, High–strength alkali–resistant sintered SiC fibre stable to 2,200°C, Nature 391 (1998) 773–775.
11. L. An, R. Riedel, C. Konetschny, H.–J. Kleebe, R. Raj, Newtonian Viscosity of Amorphous Silicon Carbonitride at High Temperature, J. Am. Ceram. Soc. 81 (1998) 1349–52.
12. P. Colombo, G. Mera, R. Riedel, G.D. Soraru, Polymer-Derived Ceramics: 40 Years of Research and Innovation in Advanced Ceramics, J. Am. Ceram. Soc. 93 (2010) 1805–1837.

13. G.D. Sorarù, S. Modena, P. Bettotti, G. Das, G. Mariotto, L. Pavesi, Si nanocrystals obtained through polymer pyrolysis, Appl. Phys. Lett. 83 (2003) 749–751.
14. M. Narisawa, M. Koka, A. Takeyama, M. Sugimoto, A. Idesaki, T. Satoh, H. Hokazono, T. Kawai, A. Iwase, In-situ monitoring of ion-beam luminescence of Si-O-C(-H) ceramics under proton-beam irradiation, J. Jap. Ceram. Soc. 123 (2015) 805–808.
15. J. Cordelair and P. Greil, Electrical Conductivity Measurements as a Microprobe for Structure Transitions in Polysiloxane Derived Si–O–C Ceramics, J. Eur. Ceram. Soc. 20 (2000) 1947–1957.
16. V.L. Nguyen, C. Zanella, P. Bettotti, G.D. Sorarù, Electrical Conductivity of SiOCN Ceramics by the Powder-Solution-Composite Technique, J. Am. Ceram. Soc. 97 (2014) 2525–2530.
17. L. Zhang, Y. Wang, Y. Wei, W. Xu, D. Fang, L. Zhai, K. –C. Lin, L. An, A Silicon Carbonitride Ceramic with Anomalously High Piezoresistivity, J. Am. Ceram. Soc. 91 (2008) 1346–1349.
18. A.M. Wilson, G. Zank, K. Eguchi, W. Xing, J.R. Dahn, Pyrolysed silicon-containing polymers as high capacity anodes for lithium-ion batteries, J. Power Sources 68 (1997) 195–200.
19. L. Ferraioli, D. Ahn, A. Saha, L. Pavesi, and R. Raj, Intensely Photoluminescent Pseudo-Amorphous SiliconOxyCarboNitride Polymer–Ceramic Hybrids, J. Am. Ceram. Soc. 91 (2008) 2422–2424.
20. A. Karakuscu, R. Guider, L. Pavesi and G.D. Sorarù, White luminescence from sol-gel derived SiOC thin films, J. Am. Ceram. Soc, 92 (2009) 2969–2974.
21. L. Liew, V. M. Bright, R. Raj, A novel micro glow plug fabricated from polymer-derived ceramics: in situ measurement of high-temperature properties and application to ultrahigh-temperature ignition, Sensors Actuators A-Physical, 104 (2003) 246–262.
22. R. Riedel, L. Toma, E. Janssen, J. Nuffer, T. Melz, H. Hanselka, Piezoresistive Effect in SiOC Ceramics for Integrated Pressure Sensors, J. Am. Ceram. Soc. 93 (2010) 920–924.
23. J. Grossenbacher, M. Gullo, F. Dalcanale, G. Blugan, J. Kuebler, S. Lecaude, H.T. Stahel, J. Brugger, Cytotoxicity evaluation of polymer-derived ceramics for pacemaker electrode applications, J. Biomed. Mater. Res. Part A 103 (2015) 3625–3632.

24. A. Karakuscu, A. Ponzoni, P.R. Aravind, G. Sberveglieri, G.D. Soraru, Gas sensing behavior of mesoporous SiOC glasses, J. Am. Ceram. Soc., 96 (2013) 2366–2369.
25. H. Fukui, H. Ohsuka, T.Hino, K. Kanamura, A Si−O−C Composite Anode: High Capability and Proposed Mechanism of Lithium Storage Associated with Microstructural Characteristics, Appl. Mater. Interfaces 2 (2010) 998–1008.
26. V.S. Pradeep, E. Zera, M. Graczyk-Zajac, R. Riedel, G.D. Soraru, Structural Design of Polymer Derived SiOC Ceramic Aerogels for High-rate Li-ion Storage Applications, J. Am. Ceram. Soc. 99 (2016) 2977–2983.
27. X. Yao, S. Tan, Z. Huang, D. Jiang, Effect of recoating slurry viscosity on the properties of reticulated porous silicon carbide ceramics, Ceram. Internat. 32 (2006) 137–142.
28. X. Bao, M.R. Mangrejo, M.J. Edirisinghe, Preparation of silicon carbide foams using polymeric precursor, J. Mat. Sci. 35 (2000) 4365–4372.
29. M.R. Mangrejo, X. Bao, M.J. Ediringhe, The structure of ceramic foams produced using polymeric precursor, J. Mat. Sci. Lett. 19 (2000) 787–789.
30. M.R. Mangrejo, M.J. Edirisinghe, Porosity and strength of silicon carbide foams prepared using preceramic polymers, J. Por. Mat. 9 (2002) 131–140.
31. S. Yajima, J. Hayashi, M. Omori, K. Okamura, Development of a silicon carbide fiber with high tensile strength, Nature 261(1976) 683–685.
32. E. Zera, R. Campostrini, P. Ramaswamy Aravind, Y. Blum, G.D. Soraru, Novel SiC/C Aerogels Through Pyrolysis of Polycarbosilane Precursors, Adv. Eng. Mater. 16 (2016) 814–819.
33. P. Jana, V. Fierro, A. Celzard, Ultralow cost reticulated carbon foams from household cleaning pad wastes, Carbon 62 (2013) 510–520.
34. S. Farhan, R. Wang, H. Jiang, K. Li, Use of waste rigid polyurethane for making carbon foam with fire proofing and anti-ablation properties, Materials and Design 101 (2016) 332–339.
35. P. Jana, M.C. Bruzzoniti, M. Appendini, L. Rivoira, M. Del Bubba, D. Rossini, L. Ciofi, G.D. Sorarù, Processing of polymer-derived silicon carbide foams and their adsorption capacity for nonsteroidal anti-inflammatory drugs, Ceram. Internat. DOI: http://dx.doi.org/10.1016/j.ceramint.2016.09.045.

36. G.D. Soraru, R. Campostrini, A.A. Ejigu, E. Zera, P. Jana, Processing and characterization of polymer derived SiOC foam with hierarchical porosity by HF etching, J. Ceram. Soc. Jpn. 124 (2016) 1023-1029.
37. F. Dalcanale, J. Grossenbacher, G. Blugan, M. R. Gullo, A. Lauria, J. Brugger, H. Tevaearai, T. Graule, M. Niederberger, J. Kuebler, Influence of carbon enrichment on electrical conductivity and processing of polycarbosilane derived ceramic for MEMS applications, J. Europ. Ceram. Soc. 34 (2014) 3559–3570.
38. ERG: Duocel®, USA, Silicon Carbide Foam, www.ergaerospace.com/SiC-properties.htm (accessed 23.09.2016).
39. L.J Gibson, M.F Ashby, Cellular solids: Structure and properties, 2nd ed., Cambridge University Press, 1997.
40. Z. Li, Y. Wang, L. An, Control of the thermal conductivity of SiC by modifying the polymer precursor, J. Euro. Ceram. Soc. 37 (2017) 61–67.
41. S. S. Hossain, S. Sarkar, N. K. Oraon, A. Ranjan, Pre-ceramic Polymer-derived open/closed cell silicon carbide foam: microstructure, phase evaluation, and thermal properties, J. Mater. Sci. 51 (2016) 9865-9878.
42. G. M. Renlund, S. Prochazka and R. H. Doremus, Silicon oxycarbide glasses: Part II. Structure and properties, J. Mater. Res. 6(1991) 2723-2734.
43. G.D. Sorarù, E. Dallapiccola, G. D'Andrea, Mechanical Characterization of Sol-Gel-derived Silicon Oxycarbide Glasses, J.Am. Ceram. Soc.79 (1996) 2074-80.
44. N. Suyal, T. Krajewski, M. Mennig, Sol-Gel Synthesis and Microstructural Characterization of Silicon Oxycarbide Glass Sheets with High Fracture Strength and High Modulus, J. Sol-Gel Sci. Technol. 13, (1998) 995–999.
45. S.R. Shah, R. Raj, Mechanical properties of a fully dense polymer derived ceramic made by a novel pressure casting process, Acta Mater. 50 (2002) 4093–4103.
46. A. Ortona, S. Gianella, D. Gaia, SiC Foams for High Temperature Applications, in: R. Narayan, P. Colombo, S. Widjaja and D. Singh (EDs.) Advances in Bioceramics and Porous Ceramics IV: Ceramic Engineering and Science Proceedings, John Wiley & Sons, Inc., Hoboken, NJ, USA, pp 153–161.
47. Ultramet Advanced Materials Solutions, USA, Refractory Open–Cell Foams: Carbon, Ceramic, and Metal, http://www.ultramet.com/refractoryopencells_properties_of_foam.html (accessed

23.09.2016).